Preparation of Novel Polymer Hybrids from Imogolite Nanofiber

K. YAMAMOTO, H. OTSUKA,
and A. TAKAHARA

[Review Article]
Vol. 39, No. 1, pp 1–15 (2007)

This review paper introduces the preparation of polymer hybrid materials from imogolite nanofiber by two different approaches. In order to realize the fine dispersion of imogolite in polymer matrix, poly(vinyl alcohol)/imogolite hybrids were prepared by *in situ* synthesis method of imogolite in polymer solution. In addition, through utilizing the strong interaction between phosphoric acid group and Al–OH on the surface of imogolite, poly(methyl methacrylate)/imogolite hybrid and enzyme/imogolite hybrid gel were prepared.

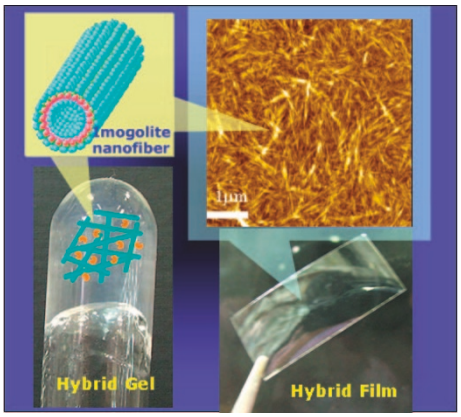

Regulation of Self-assembling Process of a Cationic β-Sheet Peptide by Photoisomerization of an Anionic Azobenzene Derivative

T. KOGA, M. USHIROGOCHI,
and N. HIGASHI

[Short Communication]
Vol. 39, No. 1, pp 16–17 (2007)

A novel photo-responsive supramolecular system has been fabricated, in which the self-assembling process of the cationic amphiphilic peptide into β-sheet nanofibers is regulated by photoisomerization of the exogenous anionic azobenzene derivative.

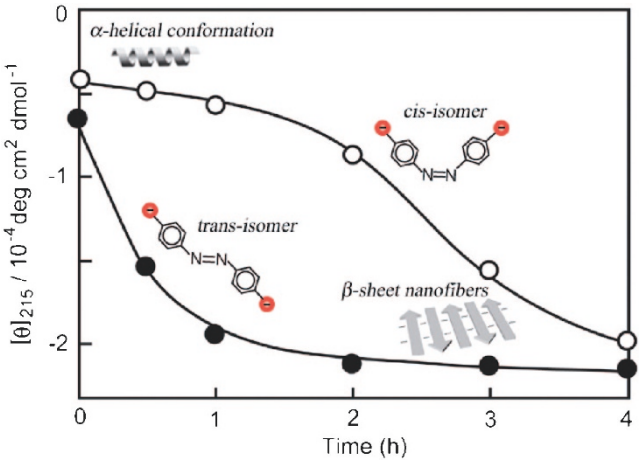

Synthesis of Nonporous Poly(*N*-alkylacrylamide) Gel Beads by Nonaqueous Sedimentation Polymerization

T. IIZAWA, T. ISHIDO, T. GOTOH,
and S. SAKOHARA

[Short Communication]
Vol. 39, No. 1, pp 18–20 (2007)

Nonaqueous sedimentation polymerization of droplets of a *N*-isopropylacrylamide (NIPA) solution in *N*-methyl-2-pyrolidinone (NMP) was conducted. The typical photographs of the obtained poly(*N*-isopropylacrylamide) beads (G-5) are shown in comparison with the shrunken beads (G-9) obtained from the conventional sedimentation polymerization of a NIPA solution in 20 wt % aqueous *N*,*N*-dimethylformamide solution. The nonporous G-5 beads are transparent, while the porous G-9 beads are opaque. When NMP was used as a solvent, the nonporous millimeter-sized poly(*N*-alkylacrylamide) beads can be easily obtained by nonaqueous sedimentation polymerization.

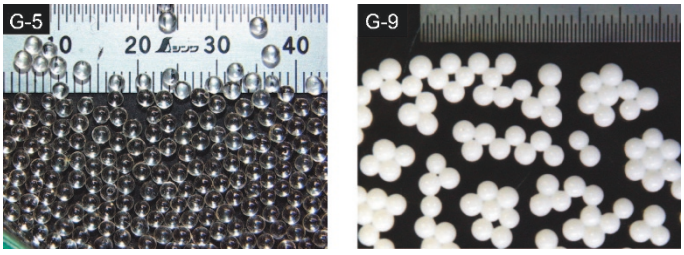

Solvent-Free Synthesis of Unmodified Cyclodextrin-Based Pseudopolyrotaxane and Polyrotaxane by Grinding

R. LIU, A. HARADA, and T. TAKATA

[Short Communication]
Vol. 39, No. 1, pp 21–23 (2007)

Unmodified cyclodextrin-based polyrotaxane was synthesized by grinding a mixture of a bulky electrophile as an end-capping agent and a pseudopolyrotaxane consisting of α-cyclodextrin and bis(3-aminopropyl)-terminated polytetrahydrofuran without solvent. The pseudopolyrotaxane was prepared from a mixture of the components both by grinding without solvent and by sonication in water.

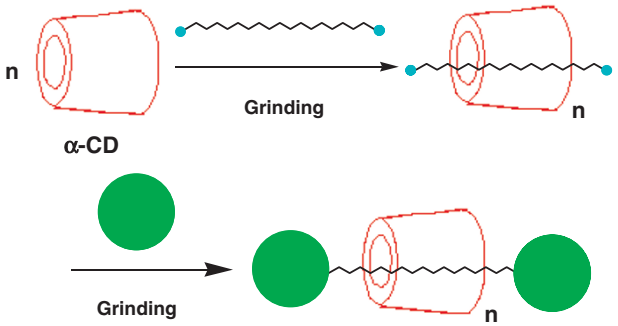

End-chain and Mid-chain Functional Macrophotoinitiators of Poly(*ε*-caprolactone) and Their Molar Mass Effects on Strong Electrorheological Response

H. YILMAZ, M. DEĞİRMENCİ, Ü. YILMAZ, and H. I. UNAL

[Regular Article]
Vol. 39, No. 1, pp 24–33 (2007)

In this study, electrical and ER properties of end-chain and mid-chain functional macrophotoinitiators of poly(*ε*-caprolactone), PCL, were investigated. For this purpose 4 different samples of PCL were synthesized with different molar masses. They were then ground milled for a few hours to obtain micron size. The particle sizes of the PCL's were determined by dynamic light scattering. Further, the effects of suspension concentration, molar mass of the PCL's, shear rate, electric field strength, frequency, promoter and temperature onto ER activities of suspensions were investigated.

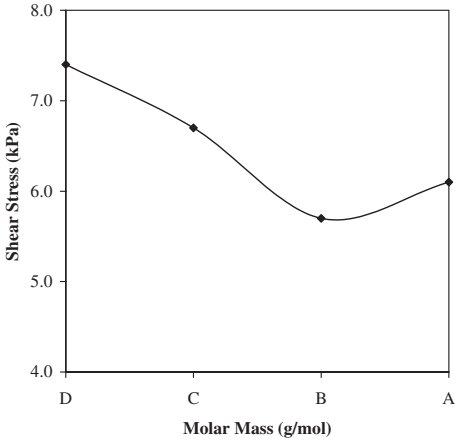

Structure of Regenerated Cellulose Films from Cellulose/Aqueous NaOH Solution as a Function of Coagulation Conditions

G. YANG, H. MIYAMOTO, C. YAMANE, and K. OKAJIMA

[Regular Article]
Vol. 39, No. 1, pp 34–40 (2007)

The structure of regenerated cellulose films from cellulose/aqueous sodium hydroxide solution was investigated by X-ray diffraction and viscoelastic measurements. In the viscoelastic measurements, four kinds of dynamic absorption peaks or shoulders were observed, named α_1, α_{sh}, β_a and γ. The analyses of peak temperatures (T_{max}) and peak intensities ($\tan\delta_{max}$) of these peaks revealed that there were two different kinds of amorphous regions.

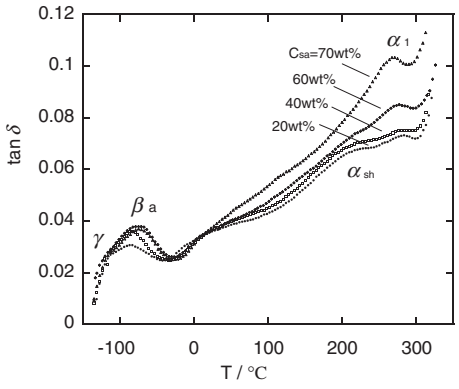

Mechanical loss tangent δ tan δ-temperature T curves of cellulose films prepared by various coagulation conditions. Numerals denote sulfuric acid concentration as coagulants.

Electroless Copper Plating onto Polyimide Using Polymer Nanosheet as a Nano-Adhesive

J. MATSUI, K. KUBOTA, Y. KADO, and T. MIYASHITA

[Regular Article]
Vol. 39, No. 1, pp 41–47 (2007)

The photoreactive polymer nanosheets were used as nano-adhesion to attached electrolessly plated copper film onto a polyimide surface. The plated copper showed strong adhesion to a polyimide film. Moreover, micrometer copper lines were fabricated by photopatterning the polymer nanosheets. The process using polymer nanosheets as an adhesive required no surface modification of polyimide substrate and enabled microscale copper line fabrication without discharging harmful waste.

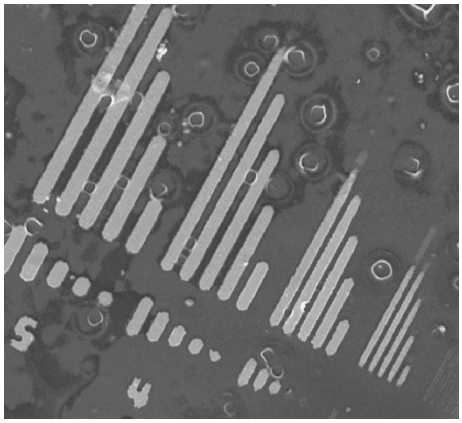

Role of Stearic Acid in Preparing EPDM/Clay Nanocomposites by Melt Compounding

Y. MA, Q.-F. LI, L.-Q. ZHANG, and Y.-P. WU

[Regular Article]
Vol. 39, No. 1, pp 48–54 (2007)

EPDM/organic clay (OC) nanocomposites were prepared by melt blending. XRD results showed that macromolecules are difficult to directly intercalate into the OC interlayers, while under pretreating conditions (S-OC) with SA, stearic acid (SA) could easily intercalate into the interlayers, and expand the space to 3.9 nm. TEM observation showed OC pretreated with SA improved the dispersion of OC in EPDM. FT-IR results indicated that the esterification reaction between carboxyl groups of SA and hydroxyl groups of OC occurred, which was believed to be the driving force of SA intercalation.

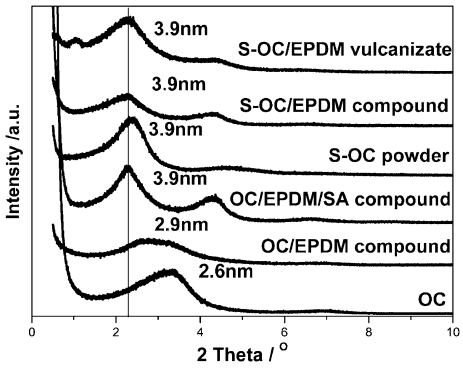

Acceleration Mechanism of Nucleation of Polymers by Nano-sizing of Nucleating Agent

T. URUSHIHARA, K. OKADA, K. WATANABE, A. TODA, E. TOBITA, N. KAWAMOTO, and M. HIKOSAKA

[Regular Article]
Vol. 39, No. 1, pp 55–64 (2007)

Acceleration mechanism of nucleation of polymers by nano-sizing of nucleating agent (NA) was solved based on kinetic study. Theoretical prediction in our previous study that $I \propto I_0 \propto C_{NA} a_{NA}^{-1}$ was confirmed, where I is nucleation rate of polymers, I_0 is prefactor, C_{NA} is a concentration of NA and a_{NA} is lateral size of NA crystal. It is concluded that decreasing a_{NA} from the order of μm to nm and narrowing distribution of a_{NA} are the most effective method to improve the nucleating ability of NA (Figure).

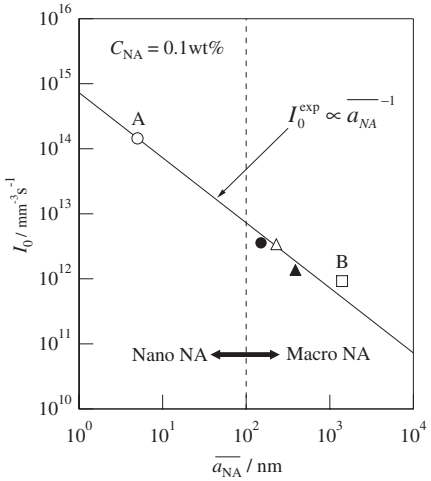

Electrospinning of Cellulose Acetate in Solvent Mixture *N*,*N*-Dimethylacetamide (DMAc)/Acetone

H. LIU and C. TANG

[Regular Article]
Vol. 39, No. 1, pp 65–72 (2007)

Cellulose acetate nanofibers with mean diameter of 345 nm were generated from 25 wt % CA in 2:1 (v/v) DMAc/acetone by means of electrospinning technique. The critical chain entanglement concentration (Ce) for the electrospinning of CA in solvent DMAc/acetone highly depends on the composition ratio of each component. Ce substantially decreased with the increasing of component acetone in the solvent mixture. CA nanofibrous membrane with relatively uniform fiber structure and diameter less than 500 nm showed hydrophilic characteristic.

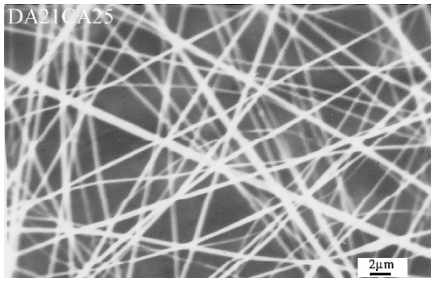

Molecular Dynamics Study of the Adhesion between End-Grafted Polymer Films II —Effect of Grafting Density—

H. MORITA, H. MIURA, M. YAMADA, T. YAMAGUCHI, and M. DOI

[Regular Article]
Vol. 39, No. 1, pp 73–80 (2007)

Adhesion between two polymer films consisting of end grafted polymer is studied by coarse-grained molecular dynamics. In this study, we discuss the effect of the grafting density along our previous study (*Polymer Journal*, **37**, 782, (2005)). Three kinds of failure patterns; fibril, cavity and brittle failures can be obtained. The maximum adhesion stress and the adhesion energy are also obtained from our MD simulations and these behaviors are strongly dependent on the temperature and the grafting density.

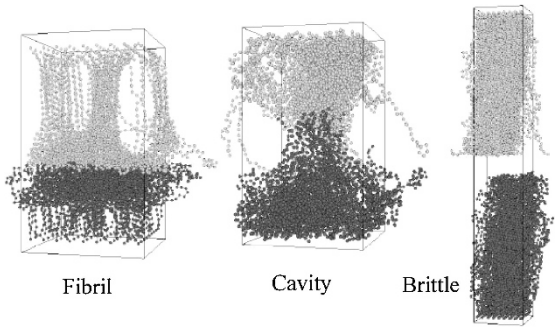

Highly Transparent Photosensitive Polybenzoxazole: Poly(*o*-hydroxy amide) Derived from 4,4′-(Hexafluoroisopropylidene)bis(*o*-aminophenol) and *o*-Substituted Dicarboxylic Acid Chlorides

Y. SHIBASAKI, F. TOYOKAWA, S. ANDO, and M. UEDA

[Regular Article]
Vol. 39, No. 1, pp 81–89 (2007)

A novel poly(*o*-hydroxyamide) (PHA) as a precursor of photosensitive polybenzoxazole (PSPBO) that exhibits high transparency at 365 nm wavelength (*i*-line) has been developed. Time-dependent density functional theory (TD-DFT) calculations using the B3LYP hybrid functional were performed to predict the transparencies of various *o*-hydroxyamides in the *i*-line region. Based on these results, several dicarboxylic acid chlorides were prepared and polymerized with 4,4′-(hexafluoroisopropylidene)bis(*o*-aminophenol). The resulting PHA-**3** showed a high transparency (92%, 1.0×10^{-3} mol/L in *N*,*N*-dimethylacetamide (DMAc)), superior to that of the conventional PHA-**1** (83% at the same concentration in DMAc) derived from 4,4′-oxybis(benzoyl chloride) in transparency. The positive-type PSPBO was then formulated based on PHA-**3** with a cross-linker and a photoacid generator, and the resulting polymer film (1.5 μm-thick) demonstrated the high photosensitivity and contrast of 32 mJ/cm^2 and 7.2, respectively.